Flux Measurement Using Aircraft and Radars

Peter H. HILDEBRAND

National Center for Atmospheric Research
P.O. Box 3000, Boulder CO 80307-3000 - U.S.A.

1.0 Measurement Goals

Aircraft are excellent platforms for measuring atmospheric turbulence. Due to their mobility and instrumentation, aircraft can make a wide variety of measurements over a large domain in a short length of time, and the aircraft flight pattern can be easily adjusted to accommodate to changes in the atmosphere and new measurement techniques.

This paper will discuss the use of instrumented aircraft to measure bulk and turbulent atmospheric transport of heat, moisture, and momentum over large distances. The paper will cover flux measurement from aircraft, the design of aircraft flight patterns. and the measurement accuracies which can result from these measurement techniques.

The measurement techniques include the use of in-situ and remote sensors. The discussion will cover aircraft instrumentation, instrumentation accuracies, the eddy correlation technique for measurement of atmospheric turbulence, and aircraft flight patterns. The discussion will be directed to particular problem of measuring the variability of atmospheric transport within an inhomogeneous atmosphere. This problem is of particular importance to TOGA COARE.

Most experiments which are designed to measure atmospheric transport of heat, moisture, and momentum have had smaller measurement domains than TOGA COARE. The TOGA-COARE time and space scales (Table 1) range from the diurnal cycle (24h and a cluster scale of about 500km), through the cloud cluster scale (1-3 days and up to 1700 km movement) to the meso-scale convective super cluster (MCC) scale (about 10 days and up to 4000 km movement). Making airborne in-situ and Doppler radar measurements over these large time and space scales will require new approaches to the collection and analysis of aircraft data.

---

[1] The National Center for Atmospheric Research is supported by the National Science Fountation.

Table 1. The TOGA-COARE observational domains.

Large Scale: (LSA)	10°N - 10°S by 140°-180°E or ≈ 2200x4400 km. Over this area the large scale convective and precipitation events are to be described and the net fluxes of heat, moisture and momentum are to be measured.
Equatorial-Synoptic: (ESA)	5°N - 5°S by 150°-175°E or ≈ 1100x2800 km. Over this area the detailed structure of convective and episodic wind events and associated precipitation fields and broad scale heat, moisture and momentum fluxes are to be measured.
Intensive Flux: (IFA)	5°N - 5°S by 155°-170°E or ≈ 1100x1700 km. This area will include very detailed determination of the surface fluxes as well as the Equatorial Synoptic area measurements.

2.0 Measurement Techniques

Aircraft are ideally suited for measuring atmospheric phenomena over large distances. Aircraft in-situ and remote probing instrumentation, coupled with long aircraft flight tracks can provide high resolution measurements over large areas. The principle measurements which can be made from aircraft include in-situ measurements of temperature, moisture, winds, pressure, cloud particles, and many atmospheric chemical constituents. In addition, research aircraft typically include measurements of short and long wave radiation, and radiative earth surface temperature. Typical in-situ aircraft instrumentation and measurement accuracies are listed in Table 2. For more information on aircraft in-situ instrumentation see Research Aviation Facility (1987a,b, 1988a,b,c).

The aircraft in-situ measurement of temperature, moisture and winds readily lend themselves to evaluation of heat and momentum fluxes within the atmospheric boundary layer. However, due to limitations on sensor sensitivity, measurements of turbulent fluxes are generally limited to boundary layer and in-cloud measurements. The concentrations and turbulent transport of some chemical species have also been evaluated (e.g. see Lenschow, et al., 1982).

Currently available remote probing measurements from research aircraft include in-cloud precipitation and wind measurements from Doppler radars, boundary layer structure and wind measurements from lidar, and sea surface properties measured using

Table 2. HAPEX King Air instrumentation for turbulence measurements.

Variable	Instrument	Manufacturer and Model	Performance Accuracy	Resolution
In-situ Instrumentation				
Position	Inertial Navigation	Litton LTN-51	≤1.0 Nml / flt hour	0.0014°
Static Press.	Oscillation Freq.	Rosemont 1501	± 1 mb	0.034 mb
Airspeed	Variable Capacitance	Rosemont 1221	± 0.7 mb	0.006 mb
Air Temp.	Platinum Resistance	NCAR Fast Resp	± 0.05 °C	0.006 °C
Air Temp.	Platinum Resistance	Rosemont 102	± 0.5 °C	0.006 °C
Humidity	Lyman-alpha Hygrometer	NCAR LA-3	± 5 %[2]	0.2 %
Humidity	Thermoelectric Hygrometer	EG&G 137-C3-S3	± 0.5 °C if T>0 °C[3] ± 1.0 °C if T<0 °C	0.006 °C
Horiz. Winds	Gust Probe and INS	NCAR	± 0.1 m/s, t<0.6 h ±(1.0+0.5t) t in hrs	0.012 m/s
Vertical Winds	Gust Probe and INS	NCAR	± 0.1 m/s	0.012 m/s
Geometric Alt.	Radio Altimeter	Collins ALT-55	± 2-3%	0.1 m
Infrared Rad.	Pyrgeometer 4-45μm	Eppley PIR	---	0.4 W/m^2
Visible Rad.	Pyranometer 0.285-2.8 μm	Eppley PSP	---	0.4 W/m^2
Surface Temp.	Bolometeric Radiometer	Barnes PRT-5	± 1 °C	0.005 °C
Radar Measurements				
Rainfall Rate	Airborne Doppler Radar	NCAR	factor of 2	
Air Velocity	Airborne Doppler Radar	NCAR	± 1 m/s	
Ocean sfc winds	Airborne Doppler Radar	NCAR	± 2 m/s	

[2] with periodic baseline calibration.

[3] if relative humidity is > 11%

radar scatterometers. For a discussion of airborne Doppler radar measurement capabilities, see Hildebrand and Moore (1989). Airborne Doppler radar capabilities are currently under development (Hildebrand et al., 1988) and significant improvements in these capabilities are anticipated by the time of TOGA COARE.

2.1 Boundary layer fluxes of heat, moisture, momentum and passive constituents.

Measurement of atmospheric flux transport using aircraft in-situ instrumentation requires making a number of assumptions about the representativeness of the measurements to the actual state of the atmosphere. Specific assumptions include:

1) the turbulent fluctuations can be separated into mean and turbulent components from which the turbulent fluxes can be calculated,

2) the measurement of boundary layer turbulence must be an accurate sample of the domain of interest and thus representative of the true average atmospheric state within that domain,

3) the domain to be sampled must be sampled instantaneously within the domain, thus removing diurnal or temporal trends from the data.

Since most in-situ aircraft instrumentation is only capable of measuring turbulent intensities characteristic of the atmospheric boundary layer or convective storms, the following discussion will center primarily on sampling the atmospheric boundary layer.

2.1.1 Separation of in-situ measurements into mean and turbulent components.

The decomposition of turbulence measurements into mean and turbulent components (Wyngaard, 1986) is based on the assumption that for any measurements of turbulent flow, that any measured value (P) can be decomposed into mean (p) and turbulent (p') portions using the relation $P = p + p'$. This decomposition assumes that some representative mean value (p) exists and that there is process whereby the mean values (p) can be separated from the turbulent (p') portions of the flow.

Once the total flow is decomposed into mean and turbulent components, the turbulent fluxes can be calculated from averages of the turbulent components, appropriately manipulated to produce the needed products. For example, the vertical fluxes of any quantity (e.g. temperature) can be calculated as the product of T' and w' values, averaged over an appropriate interval. This technique also produces true variance

and covariance values for the means of any products such as $v_1'v_1'$ and $v_1'v_2'$, respectively, where the subscripts 1 and 2 denote different variables.

Classical use of this decomposition has assumed the atmosphere to be horizontally homogeneous, and that a single mean value or linear trend will be representative of the mean state of the atmosphere. In the undisturbed atmosphere, this assumption holds well and extensive measurements of convective boundary layer fluxes have been made. For example, temperature and moisture flux profile measurements from AMTEX (Wyngaard, et al., 1978) are shown in Fig. 1 and illustrate temperature and moisture flux measurements made using 60 km flight legs and a succession of altitudes within a 1.2 km deep boundary layer. In calculations such as this, mean values of the full flight data set were used to decompose the data into mean and turbulent portions.

The problem with the "mean value" eddy correlation technique arises when the mean value or the turbulent intensity changes along the flight track. An improved method of decomposition of the data into turbulent and mean components can be through the use of spectral decomposition or filtering of the data (Hildebrand, 1988). Using this technique, the data can be decomposed into short wavelength "turbulent" components and long wavelength "mean" components. This technique is schematically illustrated in Fig. 2 (top) where the variance of the total sample (0.27) is distributed between the variance of the mean (0.25) and the variance of the turbulent component (0.02). If the decomposition were made using the assumption of a "constant" mean value (Fig. 2 bottom), the total variance (0.27) would have been erroneously attributed to turbulence. This decomposition technique enables separating the turbulence from the mean state measurements. In its application to TOGA COARE, this technique will allow for measurement of the mean and turbulent conditions along very long flight paths which include both Meso-scale Convective Systems as well as clear areas.

Eddy correlation flux measurements have been extended to some chemical species for which there exists fast response instrumentation for sampling the chemical species. For example, Lenschow, et al., (1982) have sampled vertical ozone flux over land and over the oceans.

2.1.2 Accuracy of in-situ turbulent flux measurements.

The spectrum of turbulence can be divided into components or ranges (Wyngaard, 1986). The large-scale, energy-containing eddies perform the majority of the turbulent transport in the convective boundary layer and have spectral peaks typically at about 1.5h, where h in the boundary layer depth. These large eddies are highly variable in intensity, space, and time. Accurate measurement of boundary layer turbulence requires sampling

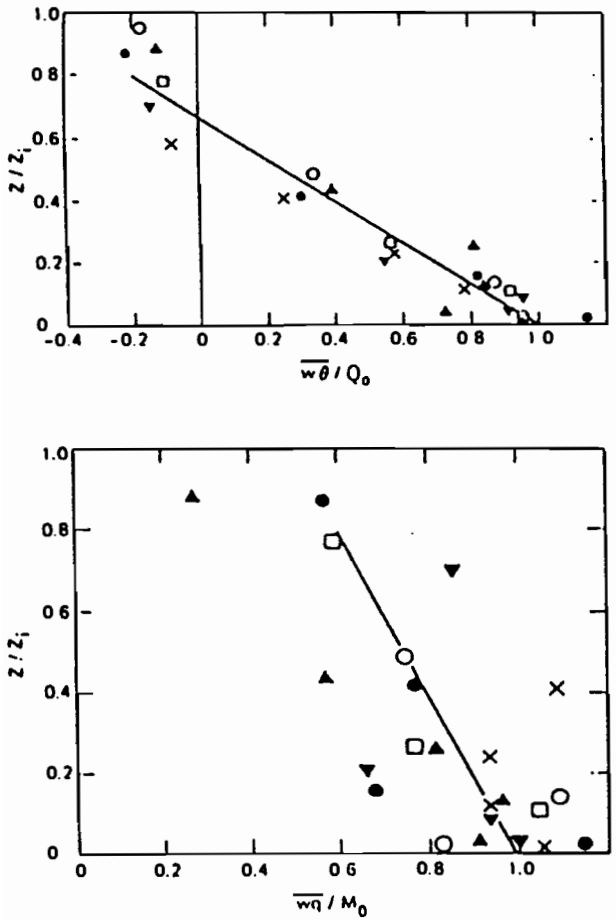

FIG.1. Measurements of the temperature and moisture flux profiles from the AMTEX experiment (after, Wyngaard et al., 1978).

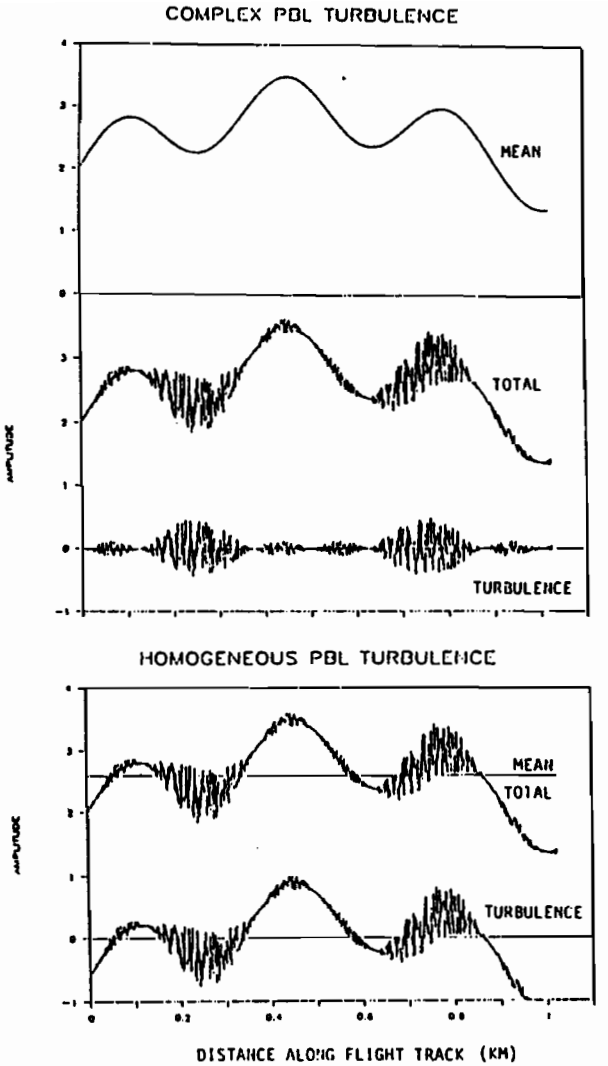

FIG.2. Top: Simulation of turbulent flow showing decomposition of the total flow into a constant mean value, plus a turbulent component having large and small scale deviations from the mean. Bottom: simulation of turbulent flow showing decomposition of the total flow through filtering into a variable mean value, plus a turbulent component only small scale deviations from the mean.

a reasonably large number of these large eddies in order to attain an accurate measurement of the boundary layer turbulence. Due to the size of the large eddies and the need to sample a number of them, flight tracks need to be fairly long if accurate turbulence measurements are to be made. This is because the turbulence measurements along the narrow flight path must be representative of a true mean value over the full boundary layer. Lenschow and Stankov (1986) evaluate the accuracy of boundary layer turbulence estimates due to random sampling error as a function of aircraft flight path length. Their relations are plotted in Fig. 3 for $0.1<z_*<.9$ and for errors ranging from 10% to 50%. These curves show that flight path lengths of 10 to 100 times the convective boundary layer depth are needed to achieve a 20% error in measurement of w'T' for measurements made between altitudes of 0.1h and 0.7h. For measurements of w'q', path lengths of about 20 to 30h will be needed to achieve 20% error.

For the AMTEX observations presented in Fig. 1, the w'T' measurements should have been accurate to about 10% at 0.1h, and to about 30% at 0.7h. The moisture flux measurements should have been accurate to 10-20% throughout the boundary layer. These error estimates are in general agreement with the scatter seen in Fig 1.

For the complex terrain, HAPEX experiment (Andre, et al., 1986), some evaluations of flux measurement accuracy were calculated as a function of sample path length (Hildebrand, 1988). Turbulence and fluxes were evaluated from 10 km block averages of the high frequency filter output. Based on a very limited sample, the HAPEX analysis (Fig. 4) shows the latent and sensible heat flux errors to drop below 20% at flight path lengths of >6h to 8h, and to drop below 10% error for flight path lengths of >15h to 18h. These results are about a factor of 2 to 3 better than the results of Lenschow and Stankov (1986).

Problems with the Lyman-alpha humidity sensor produced biases of about 5-25% difference in the measured latent heat fluxes as measured by two identical sensors in HAPEX (Hildebrand, 1988). It is likely that improvements in humidity instrumentation, currently underway in the research aviation community, should correct this problem.

On the basis of this discussion, a rough guideline is that aircraft flight tracks of about 10 times the boundary layer depth will produce measurements accurate to at least 20% for low boundary layer altitudes. Flight tracks of 30h to 50h should reliably produce heat flux measurements accurate to about 10%. For adequate sampling of turbulence at higher altitudes, track lengths will have to be longer. In the context of TOGA COARE, these restrictions do not represent a problem, and measurement accuracies of 10% to 20% should be possible.

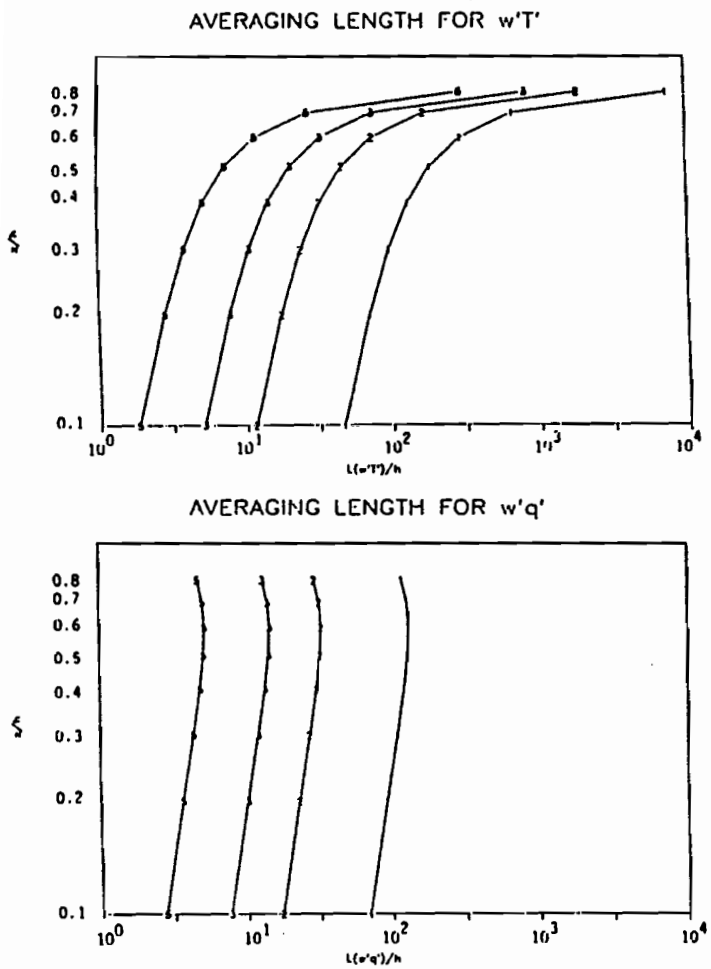

FIG.3. Vertical temperature and moisture flux accuracy as a function of flight path length and altitude in the boundary layer. The vertical scale is normalized boundary layer depth. The horizontal scale is flight path length, normalized by boundary layer depth. The curves of constant standard error of the temperature and moisture flux include 10%, 20%, 30% and 50% error curves, denoted by the number 1 through 5, respectively.

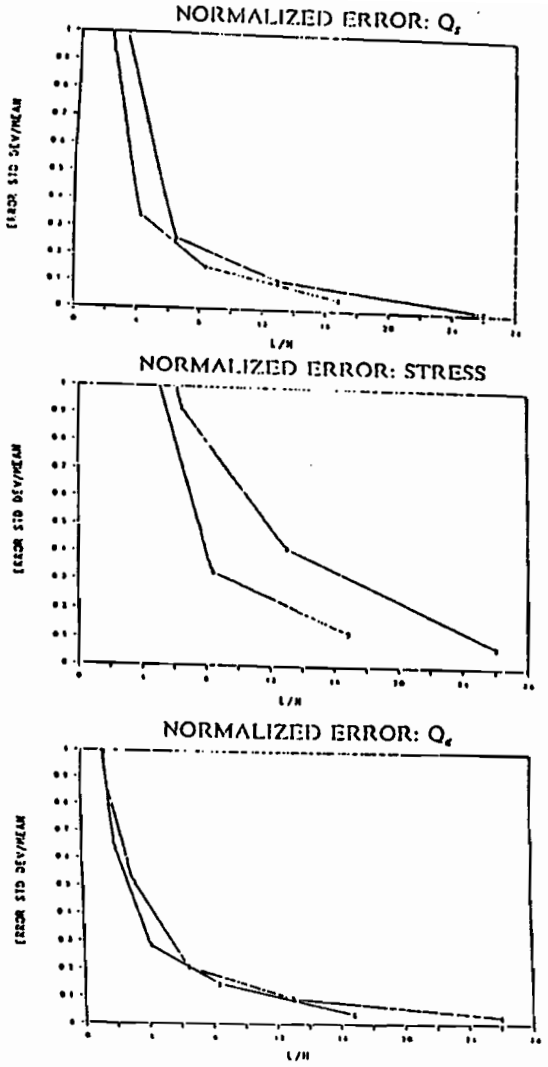

FIG.4. Measurement error plots for latent and sensible heat flux from HAPEX flight 21, for altitudes of 0.11-0.17h. The measurement error normalized by the mean value is plotted versus measurement path length normalized by the boundary layer depth.

2.1.3 Temporal effects.

During the time while observations are being made, the boundary layer is changing. This rate of change of the boundary layer is such that it can be assumed to be stationary for periods of 10 to 20 minutes. At the typical aircraft flight speeds of 120 to 150 m/s, the aircraft can fly 70 to 180 km in 10 to 20 min, depending on flight speed. The aircraft measurements can therefore be taken as approximating an instantaneous realization boundary layer turbulent flow for flight legs on the order of 30 to 100 times the typical horizontal scale length of boundary layer turbulence. For longer flight legs or repeated passes, e.g. at differing altitudes, stationarity cannot be assumed because the time required to fly the long flight leg can be long with respect to the rate of change of the boundary layer, either as the result of diurnal or other temporal forcing. This problem will have to be addressed in the design of TOGA COARE aircraft flight patterns.

2.2 Surface fluxes over the ocean

When the wind blows over the ocean surface it generates surface waves. These waves are the result of the coupling between the water surface and the drag of the wind. The surface roughness is apportionately proportional to the wind velocity. The radar backscatter cross-section of the roughened ocean surface is Bragg scattering from the surface capillary waves. This back-scattering is related to the wind speed, the incidence angle, the angle between the wind and the radar beam and radar parameters including polarization and wavelength (Ulaby et al., 1982; Elachi, 1988). The back-scatter cross section, σ_o, is given by

$$\sigma_o(U,\phi,\Theta) = A\, U^{\alpha} (1 + B \cos \phi + C \cos 2\phi)$$

where: U is the wind speed at 19.5 m msl, ϕ is the angle between the radar beam and the wind direction, Θ is the incidence angle, α is an exponent which is a function of ϕ. The constants α, A, B and C are empirically determined. Because σ is a function of U and ϕ, more than one measurement is necessary to determine the wind. Measurements from at least two orthogonal pointing angles are used to provide estimates of U with 4-fold ambiguity. This ambiguity can be resolved using synoptic meteorological analyses to select the correct quadrant. Addition of a third pointing angle at 45° to the other two can provide a measurement with a 180° ambiguity.

This technique has been used to derive surface winds over large areas of ocean. Figure 5 shows wind vector aliases for the Seasat SASS dual-beam scatterometer in the north Atlantic (Brown, 1983). Empirical evaluations of this technique (e.g. Jones, et al.,

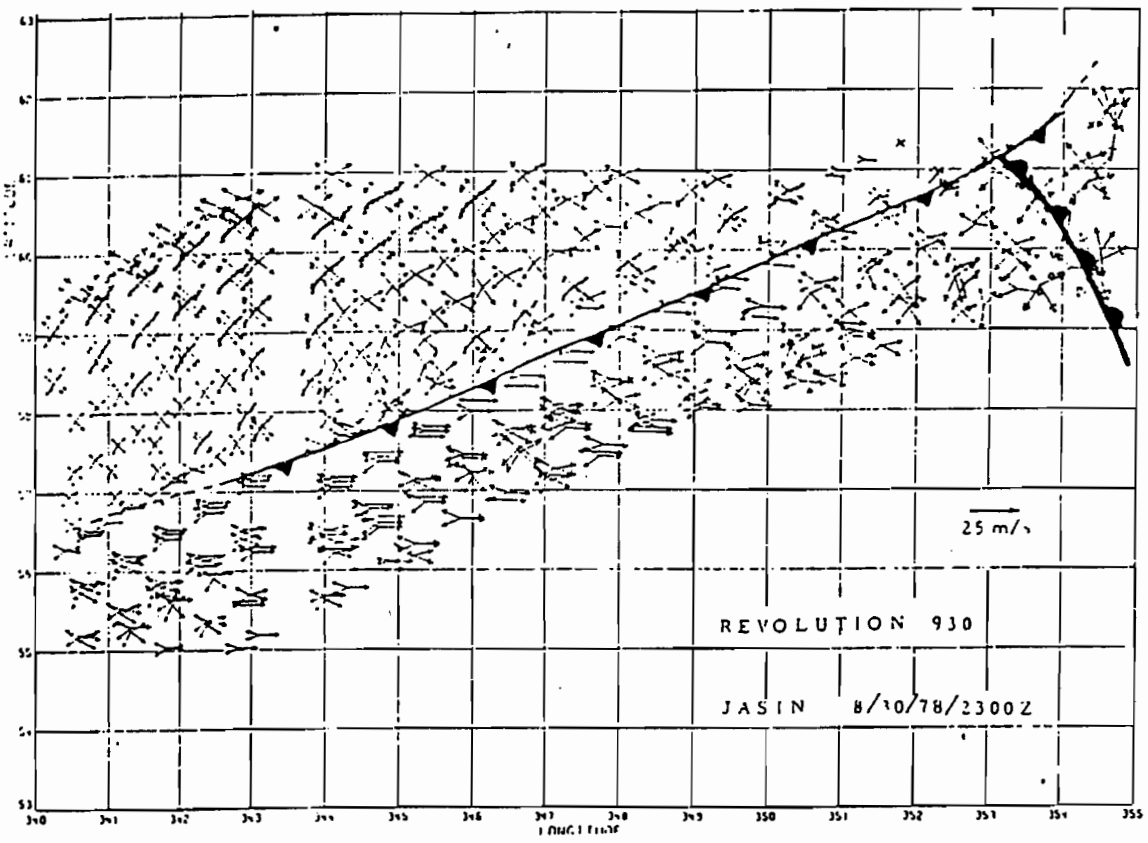

FIG.5. Wind vector alaises for the Seasat SASS dual-beam scatterometer in the north Atlantic (after Brown, 1983).

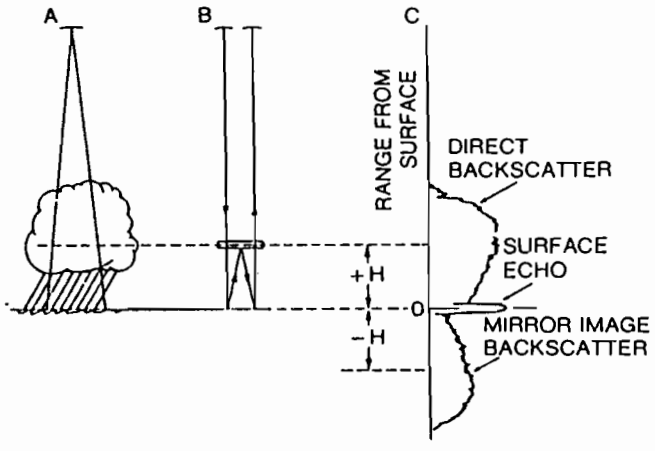

FIG.6. Use of sea surface reflection of radar measurements in rainfall to determine rainfall rate, attenuation and sea surface radar cross section. (after Meneghini and Atlas, 1984).

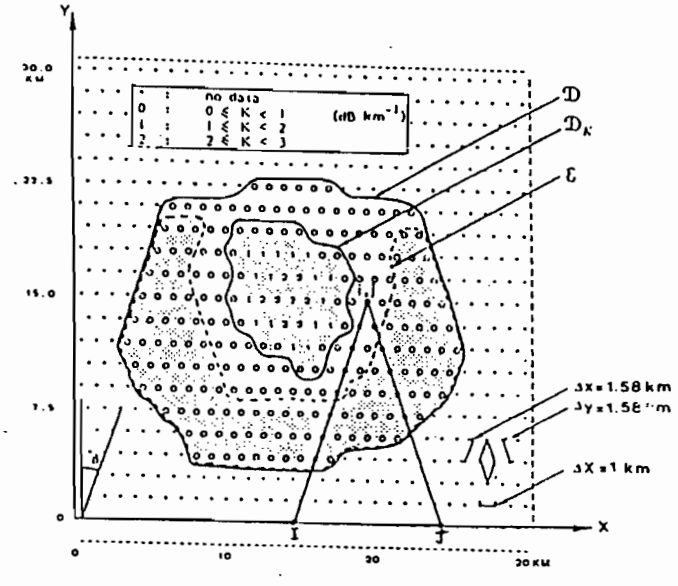

FIG.7. Stereoradar dual beam measurement of attenuation. (after Testud and Amayenc, 1988).

1978) have demonstrated that wind speeds within ±2 m/s (or about ± 10 %) and wind directions within ±20° are possible for winds of about 2 to 16 m/s. Over the ocean, the surface roughness can be related to the wind speed on the basis of simple empirical relations. The surface wind stress can therefore be derived from the 19.5m wind speed measurements. Additional research is needed, for measurement inconsistencies have been noted for high and low wind speeds and also resulting from sea surface temperature effects on viscosity (Woiceshyn, et al., 1986).

Using an airborne Doppler radar such as the ELDORA system (Hildebrand et al., 1988), surface wind and wind stress measurements can be obtained at all locations below the aircraft flight track. The data from within about ± 45° away from nadir can be used to formulate estimates of U and u* along the flight track. Such estimates can be mapped out away from the flight track to a distance approximately equal to the aircraft altitude.

Since the airborne radar also will include measurements of precipitation, it may be possible to correct the surface cross-section and wind measurements for rainfall and high wind surface spray. Additionally, the aircraft will provide radiometric surface temperature measurements, T_{SFC}. The measurements of surface temperature may enable correcting the relationship between the surface wind speed and the sea surface radar cross section for changes in T_{SFC}.

2.3 Large scale atmospheric transport through advective processes.

The advective transport of heat, moisture, and momentum can be evaluated from aircraft measurements, provided diurnal and temporal changes can be accommodated. The base measurements of atmospheric state parameters are measured accurately enough to provide quite meaningful evaluations of atmospheric gradients and advection. The temperature, humidity, and wind speed measurement accuracies (Table 2) provide advective transport measurements with accuracies of 10% to 20% for typical values of Q_s, Q_l and momentum flux. These values are comparable to the basic vertical flux measurement accuracies. However, due to the use of mean values in these calculations, the representativeness problem of the turbulent flux measurements does not affect these measurements.

The major problem in providing such measurements is related to development of a measurement technique which provides for adequate measurements and modeling of diurnal and temporal changes. For any long flight track the time required to fly the track will be long with respect to significant diurnal changes. This will require the use of fixed point measurements of diurnal or temporal changes.

2.4 Convective/MCS scale transport of heat, moisture and momentum.

Significant atmospheric heating occurs as a result of precipitation occurring in Meso-scale Convective Systems, particularly in the tropics. Measurement of precipitation production and distribution, both spatially and with altitude is therefore an important component of the TOGA COARE measurement program. The instrumented aircraft can provide accurate in-situ measurements of atmospheric dynamics and precipitation along the fight path; however, these measurements are hardly representative of the full Meso-scale Convective System transport. Therefore, use of airborne Doppler radars is essential to this measurement goal.

2.4.1 Precipitation measurement

The measurement of rainfall using radar involves use of radar reflectivity (Z) - rainfall (R) relationships in which it is assumed that $Z = aR^b$, where a and b are empirically derived constants which depend heavily on the rainfall dropsize distribution. Although these relationships are useful, they are inherently inaccurate due to the sensitivity of these relationships to the rainfall dropsize distribution. Additional radar rainfall measurement problems include incorrect radar rainfall algorithms, attenuation of the radar signal, contamination of the radar data due to partial beam filling, and the effects of ground clutter and incorrect calibration of the radar. Without additional calibration, radar rainfall measurements are subject to at least factor of two errors. Use of additional calibration (e.g. rain gages, aircraft, etc.) can provide measurements which may be as good as 10% or better for large area, long term precipitation measurement accuracies.

Improved rainfall estimation can be obtained using measurements of the attenuation (A) of the radar signal as it passes through the rainfall. This is because the A-R relations are insensitive to the rainfall particle size distribution, whereas the Z-R relations are quite sensitive to the dropsize distribution. Meneghini and Atlas (1984) have developed a technique of measuring rainfall rate and ocean surface cross section (Fig. 6). Another technique has been suggested by Testud and Amayenc (1988) in which the attenuation is determined from a dual beam airborne Doppler radar (Fig. 7). Both techniques make use of dual path precipitation observations to measure the attenuation. Either technique will enable measurement of A; hence, measurements of R of improved accuracy. A great deal of research has been devoted to development of improved remote rainfall measurement capabilities (Simpson, 1988). A major component of TOGA COARE will therefore include evaluation of these and other algorithms for improved accuracy radar rainfall measurement.

2.4.2 Storm cell/core transport processes.

Studies of cumulonimbus transport in GATE (LeMone and Zipser, 1980) and TAMEX (Jorgensen and LeMone, 1989) showed that the majority of convective drafts and cores are of scales of less than 2 km, and the primary mass transport in Meso-scale Convective Systems, also occurs at small scales (Fig. 8). In TAMEX, GATE and hurricanes only a rather small fraction of mass transport is associated with cores of >2 km or >3m/s (Jorgensen, 1984; Jorgensen and LeMone, 1989). Thus, for these cases, the narrow and weak cores are important to the vertical transport of mass.

2.4.3 Doppler radar measurement techniques

The current airborne Doppler measurements are principally suited for measurements of storm scale motions. Due to the slow scanning rate of the current airborne Doppler radar systems, the analysis of convective scale features of tropical convection has depended largely on aircraft in-situ measurements of air motions.

Measurement of the small scales of transport in tropical convection requires improvements in the resolution capabilities of airborne measurement systems. The NCAR ELDORA Airborne Doppler Radar Development Program (Hildebrand, et al., 1988) will include the improved spatial resolution as well as improved velocity and reflectivity measurement accuracy. The scanning techniques for the P-3 and ELDORA radars are illustrated in Fig. 9. The current NOAA P-3 aircraft are equipped with Doppler radars which make measurements every 1 km along the flight path (Fig. 10, bottom). A major needed improvement currently underway at NCAR will provide sampling data densities at up to 0.3 km (Fig. 10, top). The relative abilities of the P-3 and ELDORA radars to collect dual Doppler measurements of storm motions are illustrated in Fig. 11, where the areas covered in three hour flights are illustrated for the two radar systems. In large storm systems, such as the tropical storm illustrated in the lower left, some areas may be to intense to fly through. This may prohibit data collection, particularly for the P-3 radar.

3.0 Flight Patterns for Large Scale Atmospheric Flux measurements over the tropical ocean.

The seemingly diverse goals for the airborne flux measurements can very likely be accomplished with only a modest number of flight plans. The major constraints will include the flight range and duration of the aircraft, the range of operating altitudes, and the location of airports which are capable of supporting the aircraft. The flight

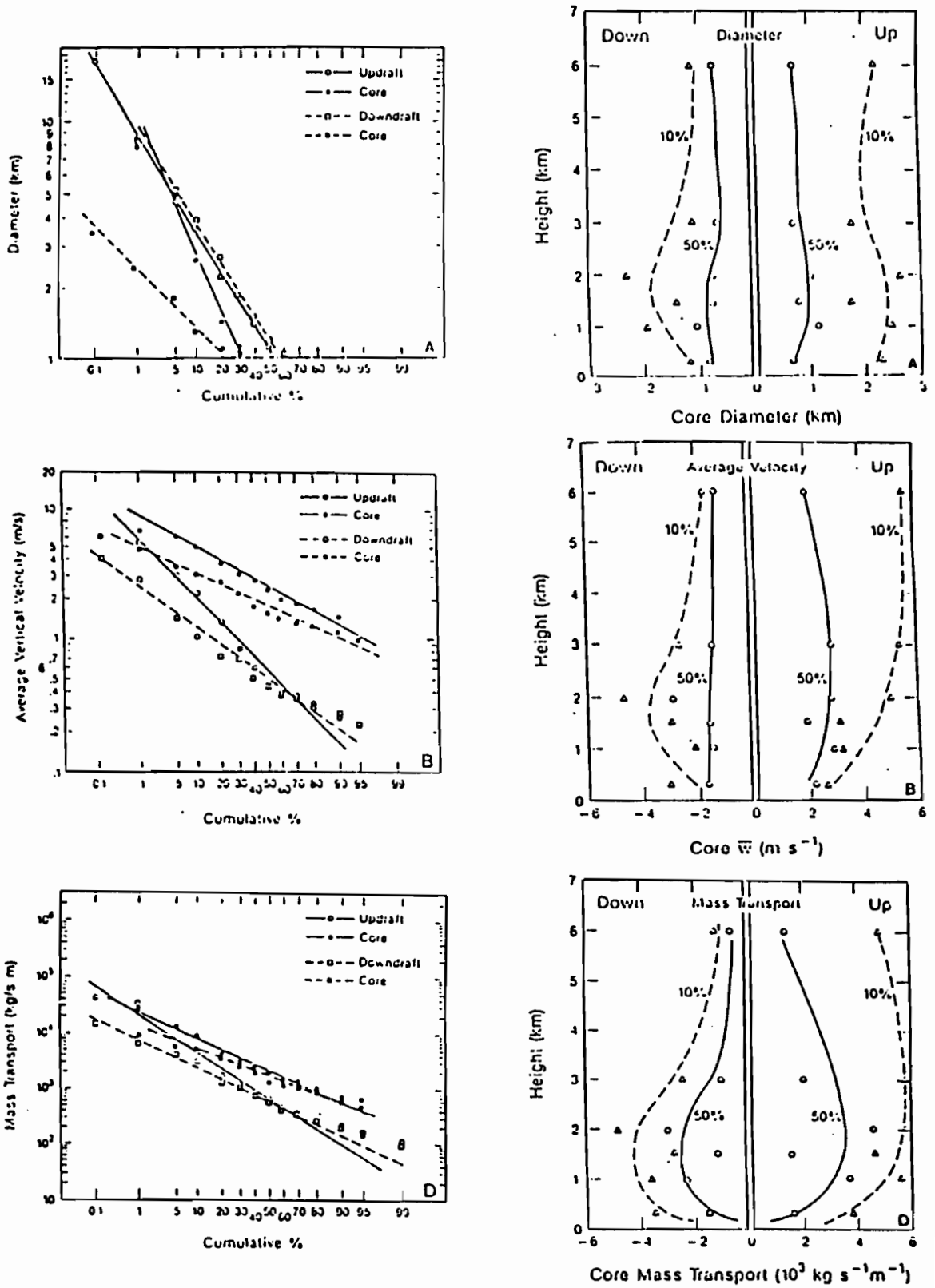

FIG.8. Left: Log-normal plots of cumulative distributions of (a) diameter, (b) average vertical velocity and (c) mass transport for MCSs. Right: Variation with altitude for the same three variables. (after Lemone and Zipser, 1980).

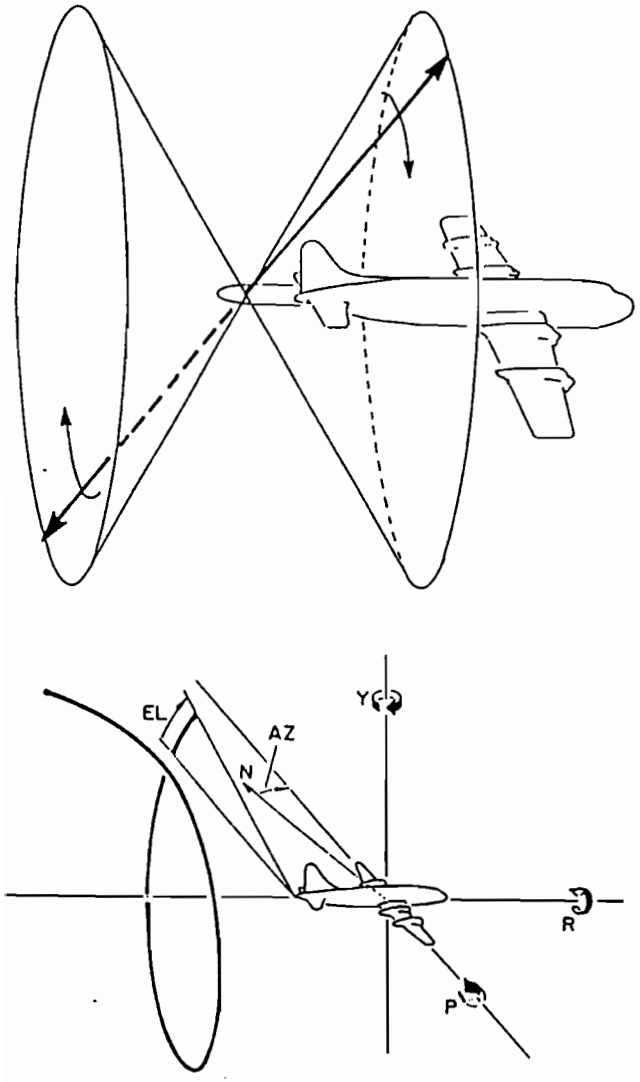

FIG.9. Scan techniques for the NCAR ELDORA (top) and NOAA P-3 airbone Doppler radars (bottom).

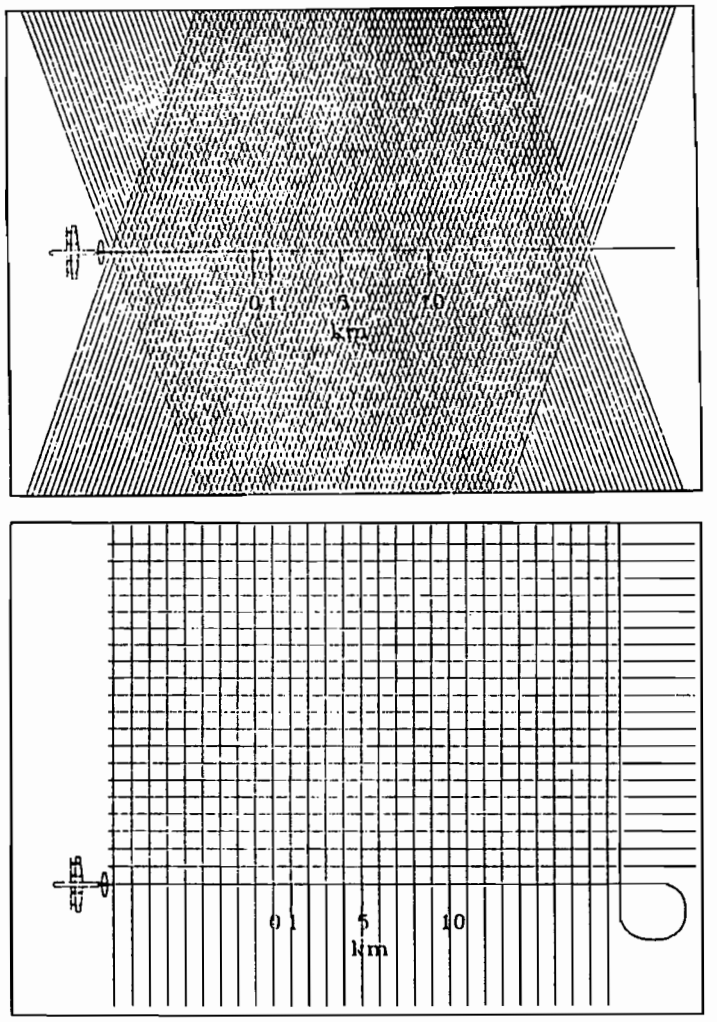

FIG.10. Horizontal measurement data density for the NCAR ELDORA (top) and NOAA P-3 airborne Doppler radars (bottom).

characteristics of the NCAR Electra and NOAA P-3 aircraft are listed in Table 3. Identification of which airfields in the TOGA COARE area have facilities which are suitable for the NCAR Electra or NOAA P-3 aircraft will be determined by NCAR and NOAA. While many of the larger islands will have airfields capable of handling the aircraft, some of these airfields may have several facilities.

Table 3. The flight characteristics of the NCAR Electra and NOAA P-3 aircraft.

Aircraft	Altitude (km)	Range (km)	Endurance (h)	Payload (kg)	Power (kw)
NCAR Electra	7.8	4,800	8	10,500	70
NOAA P-3	7.8	6,000	10	5,500	14.3

3.1 Large scale flight patterns for in-situ flux measurements

These flights will be oriented toward measurement of large scale atmospheric fluxes and gradients. Accordingly, long flight paths will be flown over large areas. These flight paths will include both Meso-scale Convective System and clear areas.

For the purpose of flux measurement, the flights will primarily be flown at altitudes in the boundary layer. Typical flights for boundary layer flux measurements (Fig. 12) will include flight leg lengths on the order of >100 km, soundings through the altitudes of interest, possible repeated flight legs at differing altitudes within the boundary layer, use of two aircraft to assess flux divergences along long flight tracks, use of multiple aircraft to assess diurnal changes over fixed flight tracks, and use of multiple aircraft to map large areas in reasonable short lengths of time. The use of cross-wind flight legs is illustrated in Fig. 12. Past studies of convective scales and sampling in the boundary layer have shown that convective large eddy scale sizes are frequently smaller in the cross-wind direction. Data collection in the cross-wind direction therefore improve sampling.

For the purpose of measuring Meso-scale Convective System structures with in-situ instrumentation or with radars, the aircraft will operate at a variety of altitudes from near sea surface to the maximum operating altitude of the aircraft. Typical flights for Meso-

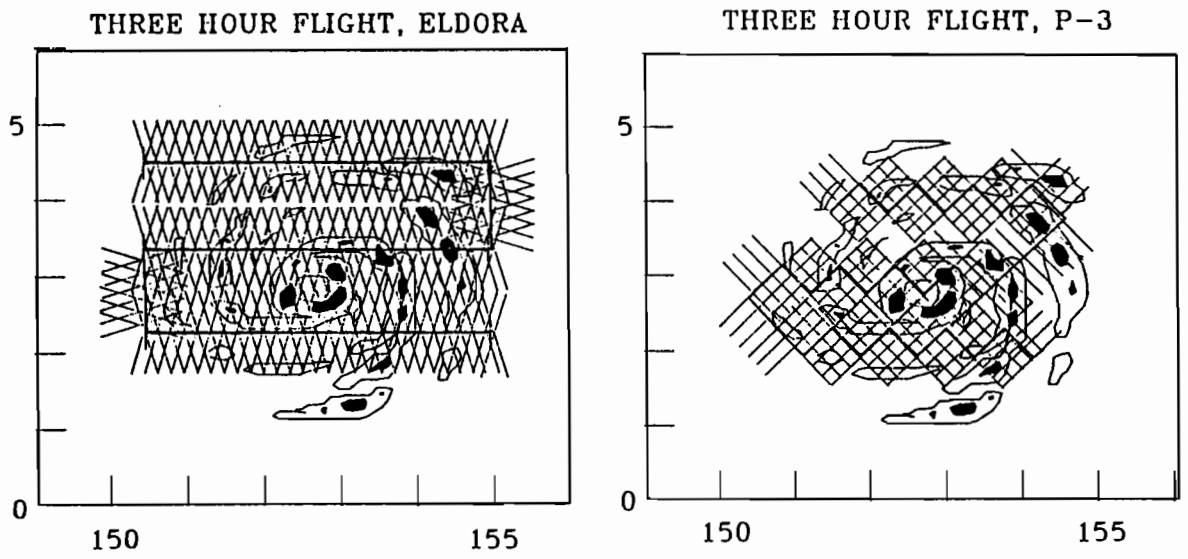

FIG.11. Three hour data collection areas for the NCAR ELDORA (right) and NOAA P-3 airborne Doppler radars (left).

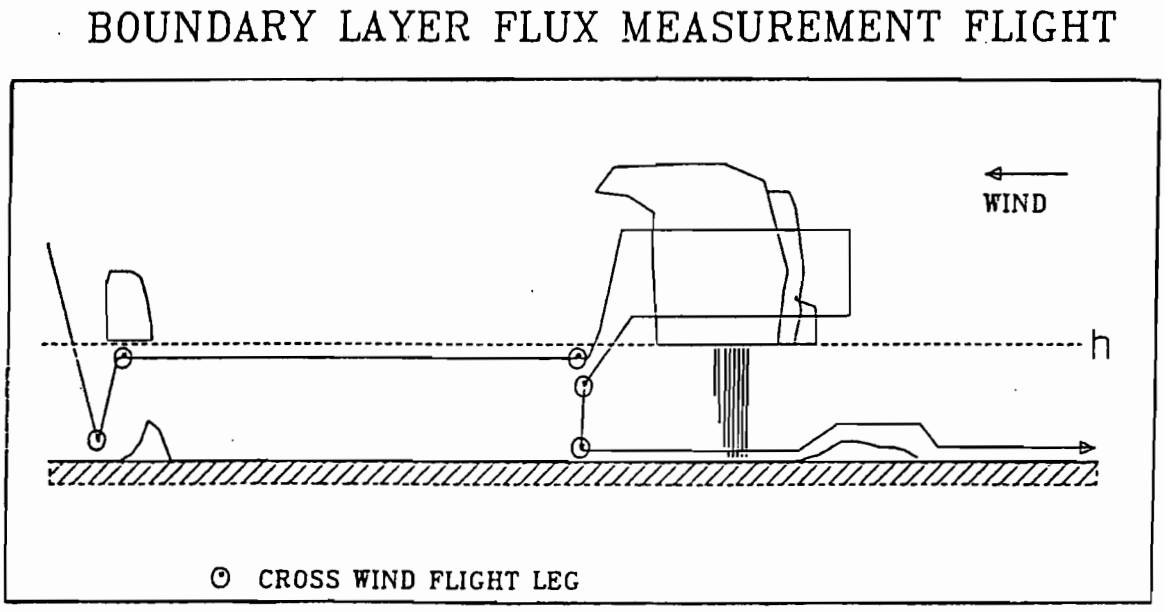

FIG.12. TOGA-COARE boundary layer flux measurement flight patterns.

scale Convective System structure measurement will include the same types of flights as for the flux measurement; however, the range of operating altitudes will be shifted to include all altitudes from the sub-cloud layer to the maximum operating altitude of the aircraft.

3.2 Airborne Doppler measurements of storm structure.

Use of the airborne Doppler radars for measurements of storm structure will vary some between the NCAR Electra and NOAA P-3 aircraft. For either type of airborne Doppler radar system, the flights can be made at a variety of altitudes according to other measurement needs (Fig. 13).

Due to the design of the NCAR ELDORA system, the Electra will be able to fly in simple straight lines through Meso-scale Convective Systems (Fig. 11). Such measurements can be made either in single paths past the storms, or in repeated flights through the storms. Since the radar only makes measurements out to about 60 km on either side of the flight track, multiple passes will be required to approach full coverage of large Meso-scale Convective Systems.

Flights using the NOAA P-3 aircraft for airborne Doppler radar measurements can be very much the same as the NCAR Electra flights, providing only single Doppler data are needed. However, the P-3 flights will be somewhat more complicated when dual Doppler data are desired. As is the case with the NCAR Electra, multiple passes will be needed to cover large Meso-scale Convective System areas.

A likely mode of operation will be to use the two aircraft in different modes. The ELDORA measurements can be directed toward dual Doppler radar and precipitation measurements of fine scales of Meso-scale Convective System motions which are related to Meso-scale Convective System transport mechanisms. The P-3 measurements can be directed toward radar measurements in which the higher resolution of ELDORA is not necessary and toward in-situ measurements. This complementary use of the aircraft will greatly enlarge the area observed in a given length of time.

3.3 Airborne radar measurement of backscatter cross-section.

The NCAR ELDORA radar, with its dual beam scanning, will provide measurements of near sea-surface (19.5m) winds and surface stress. Such measurements will be available in a swath under the aircraft extending away from the flight track

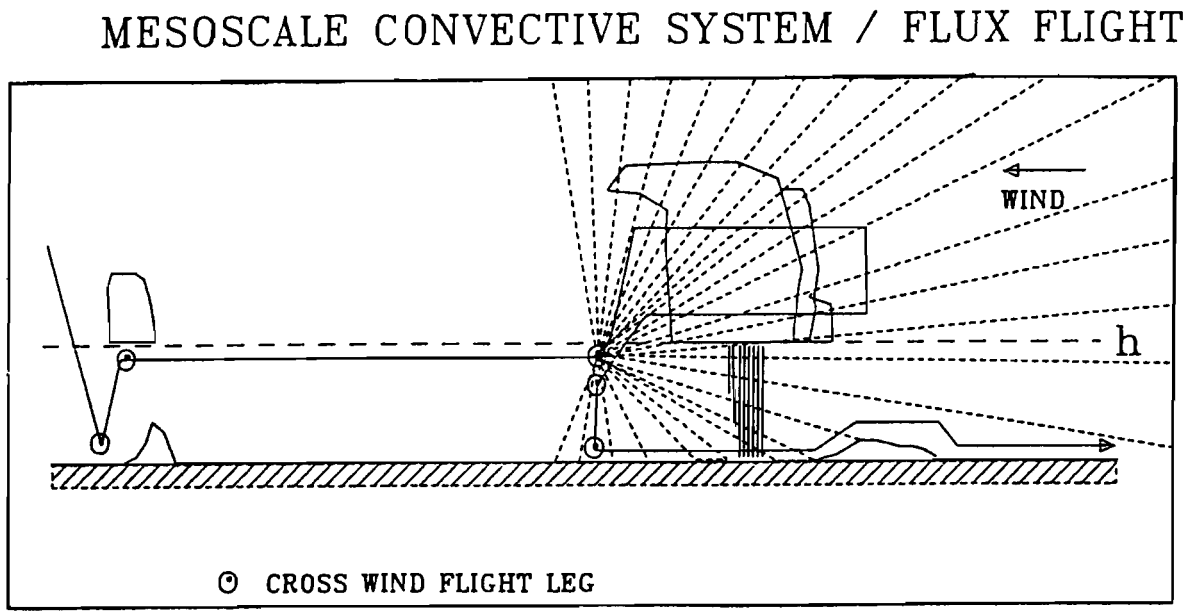

FIG.13. TOGA-COARE MCS measurement flight patterns.

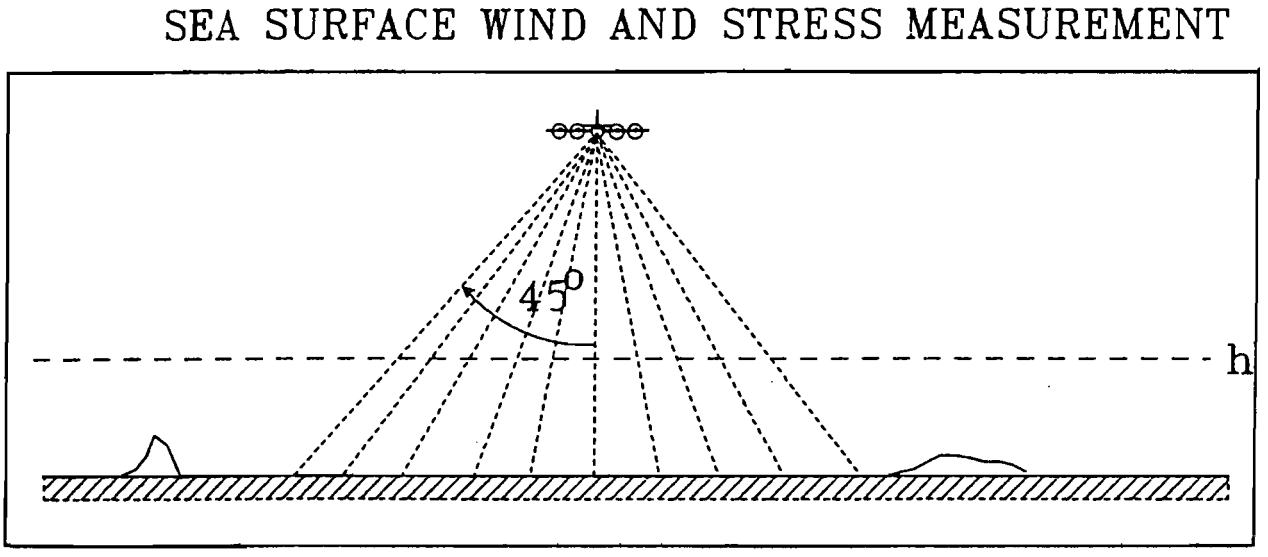

FIG.14. Airborne radar measurement of sea surface winds and stress.

approximately by the aircraft altitude (Fig. 14). The NOAA P-3 system will have some similar, but reduced accuracy abilities. There are some conflicting aspects of the use of both radar systems. Attenuation of the radar signal between the aircraft and the sea surface will deteriorate the quality of the wind and stress estimate. This error may, to some extent, be corrected by the mirror image technique of Meneghini and Atlas (1984). This possible attenuation may provide the impetus to fly fairly close to the sea surface. On the other hand, an increased altitude will widen the swath width for surface winds and stress. This goal will strongly advocate a higher altitude for radar observations.

In Meso-scale Convective System areas, the Doppler radar data are probably best collected at altitudes of 5-6 km. These altitudes will provide good swath widths. When the aircraft are being used for flux measurements, the typical 0.1-1.5 km flight altitudes will only provide surface wind and stress measurements along and very near to the flight track.

3.4 Measurements of atmospheric chemical constituents and transport.

Both the NCAR Electra and the NOAA P-3 aircraft routinely fly a wide variety of user-supplied instrumentation, much of it related to measurement of atmospheric chemistry. It is anticipated that the background state and transport of atmospheric chemical constituents may be an important ancillary role for these aircraft.

REFERENCES

Andre, J.C., J.P. Goutorbe and A. Perrier, 1986: HAPEX-MOBILHY: A Hydrologic Atmospheric Experiment for the Study of Water Budget and Evaporation Flux at the Climatic Scale, Bull. Amer. Meteor. Soc., 67, 138-144.

Brown, R.A., 1983: Surface wind analysis for SEASAT. J. Geophys. Res., 88, 1663-1673.

Elachi, C., 1988: Spaceborne Radar Remote Sensing: Applications and Techniques, IEEE Press, New York, N.Y. 254pp.

Hildebrand, P.H., C.L. Frush and C. Walther, 1988: Design of the ELDORA airborne Doppler radar. NCAR Technical Note NCAT/TN-325+EDD, 137 pp. (Category #5).

_____, 1988: Eddy correlation turbulence measurements from aircraft. Preprints, Workshop on Measurement and Parameterization of Land-Surface Evaporation Fluxes Workshop, Banyuls, France, 10-21 October 1988.

_____ and R. Moore, 1989: Meteorological radar observations from mobile platforms. Proceedings, Battan Memorial Radar Meteorology Conference. Amer. Meteor. Soc., Boston, MA, USA. (in press)

Jones, W., F. Wentz, and L. Schroeder, 1978: Algorithm for inferring wind stress form SEASAT-A. AIAA J. Spacecraft Rockets, 15, 368-374.

Jorgensen, D.P., 1984; Mesoscale and convective scale characteristics of mature hurricanes. Part I: General observations by research aircraft. J. Atmos. Sci., 42, 839-856.

Jorgensen, D.P. and M.A. LeMone, 1989: Characteristics of convective vertical velocity events observed by P-3 aircraft during TAMEX. Preprints, 18 Conf. on Hurricane Forecasting and Tropical Meteorology, San Diego., Amer. Meteor. Soc., Boston.

LeMone, M.A. and E. J. Zipser, 1980: Cumulonimbus vertical velocity events in GATE. Part I: diameter, intensity and mass flux. J. Atmos. Sci., 37, 2444-2457.

Lenschow, D.R. Pearson and B. Stankov, 1982: Measurement of Ozone vertical flux to ocean and forest. J. Geophys. Res., 87, 8833-8837.

_____ and B. Stankov, 1986: Length scales in the convective boundary layer, J. Atmos. Sci., 43, 1198-1209.

REFERENCES CONT'D

Meneghini, R. and D. Atlas, 1984: Simultaneous ocean cross-section and rainfall measurements from space with a radar pointed radar. NASA Tech. Memo. 86167, 42pp.

Research Aviation Facility, 1987a: Airborne Humidity Measurements, Research Aviation Facility, Bulletin 22, NCAR, Boulder, Co., 7pp.

Research Aviation Facility, 1987b: Measurements Techniques: Air Motion Sensing, Research Aviation Facility, Bulletin 23, NCAR, Boulder, Co., 49pp.

Research Aviation Facility, 1988a: The King Air: Overview and Summary of Capabilities, Research Aviation Facility, Bulletin 2, NCAR, Boulder, Co., 13pp.

Research Aviation Facility, 1988b: Flight Planning : King Air, Research Aviation Facility, Bulletin 5, NCAR, Boulder, Co., 7pp.

Research Aviation Facility, 1988c: Standard Output Data Products from the NCAR Research Aviation Facility, Research Aviation Facility, Bulletin 9, NCAR, Boulder, Co., 70pp.

Simpson, J., Ed., 1988: Report of the science steering group for a tropical rainfall measurement mission (TRMM), NASA Goddard Space Flight Center, Greenbelt, MD., 94pp.

Testud, J. and P. Amayenc, 1988: Stereoradar meteorology: A promising technique to observe precipitation from a mobile platform. J. Atmos. and Ocean. Technol., 6, 89-108.

Ulaby, F., R. Moore and A. Fung, 1982: Microwave Remote Sensing Vol II: Radar Remote Sensing and Surface Scattering and Emission Theory. Addisen-Wesley, Reading MA, 1064pp.

Wyngaard, J., 1986: Measurement Physics. Probing the Atmospheric Boundary Layer, ed. D. Lenschow, Amer. Meteor, Soc., Boston, 5-18.

_____, W. Pennell, D. Lenschow and M. LeMone, 1978: The temperature-humidity covariance budget in the convective boundary layer. J. Atmos. Sci., 35, 47-58.

REFERENCES CONT'D

Woiceshyn, P.M., M.G. Wurtele, D.H. Boggs, L.F. McGoldrick, and S. Peteherych, 1986: The necessity for a new parameterization of an empirical model for wind/ocean scatterometry. J. Geophys. Res., 91.

WESTERN PACIFIC INTERNATIONAL MEETING AND WORKSHOP ON TOGA COARE

Nouméa, New Caledonia
May 24-30, 1989

PROCEEDINGS

edited by

Joël Picaut *
Roger Lukas **
Thierry Delcroix *

* ORSTOM, Nouméa, New Caledonia
** JIMAR, University of Hawaii, U.S.A.

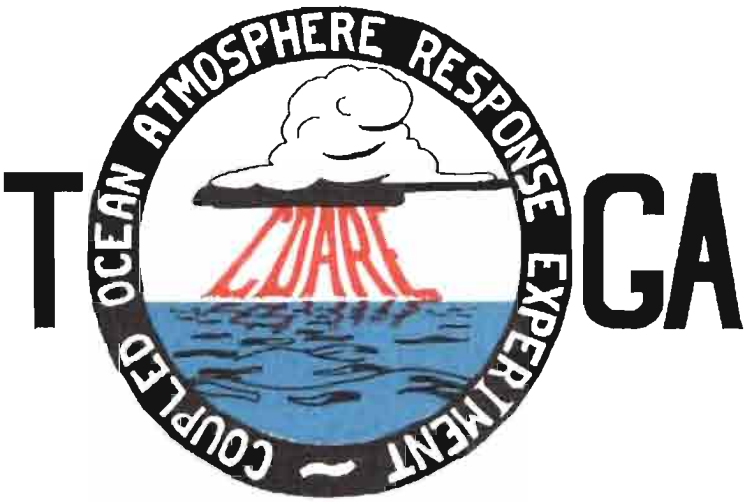

INSTITUT FRANÇAIS DE RECHERCHE SCIENTIFIQUE
POUR LE DÉVELOPPEMENT EN COOPÉRATION

ORSTOM

Centre de Nouméa

TABLE OF CONTENTS

MEETING COLLECTED PAPERS

WATER MASSES, SEA SURFACE TOPOGRAPHY, AND CIRCULATION

EL NINO/SOUTHERN OSCILLATION 1986-87

THEORETICAL AND MODELING STUDIES OF ENSO AND RELATED PROCESSES

MOMENTUM, HEAT, AND MOISTURE FLUXES BETWEEN ATMOSPHERE AND OCEAN

EMPIRICAL STUDIES OF ENSO AND SHORT-TERM CLIMATE VARIABILITY